Removal of the Finite-Distance Source Effect on the Applebaum Array

Ahmed Yamani, *Member, IEEE,* and Madina Hamiane

***Abstract*— The effect of a finite-distance signal source on the performance of an Applebaum array has been studied extensively in the literature. It has been concluded that unless the Applebaum array is focused at the exact source location, the degradation of the output signal-to-noise ratio (SNR) becomes unacceptable. The automatic focusing technique (AFT), developed for long-wavelength imaging systems using nonadaptive linear arrays, is extended to focus adaptive arrays such as the Applebaum type. Thereafter, the far-field steering vector is used successfully to form a beam toward the desired signal while suppressing the interferences. In addition, substantial improvements in data processing have been achieved through the use of a partial convolution in the frequency domain. It is also demonstrated that the AFT can be used when the signal source range lies in the beginning of the Fresnel region of a nonadaptive linear array with negligible loss in the output signal-to-noise ratio.**

I. Introduction

THE Applebaum-type adaptive array [1], [2] has many applications, such as in communication systems, radar systems, and nondestructive testing (NDT). It is capable of pointing a beam toward a desired signal direction and suppressing interferers automatically by the use of a steering vector. It has been shown [3], [4] that this type of array is highly sensitive to errors in the steering vector. Particularly when the distance between the signal source and the array center is finite, an Applebaum array is much more sensitive to the source distance than a conventional beam-forming array under far-field steering. It has also been shown [3], [4] that the far-field range of the Applebaum array is $N\gamma_d$ times that of the conventional nonadaptive beam-forming array [5], where N is the number of array elements and γ_d is the input signal-to-noise ratio per element. Thus, when the source is not at the far field, the Applebaum array needs to be focused at the location of the source. Furthermore, the range beamwidth or depth of field of the Applebaum linear array is reduced by a factor of $N\gamma_d$ [4] compared with that of a conventional, nonadaptive beam-forming array. It can be said, therefore, that for finite-distance source applications, the Applebaum array can only be used when *a priori* and exact information concerning the source location and direction is available.

In this paper, it is demonstrated that the automatic focusing technique [6], [8], developed for nonadaptive linear arrays used in long-wavelength imaging systems, can be extended to focus adaptive linear arrays at a finite and unknown source location. It is also shown that, when the signal source lies at the beginning of the Fresnel region [12] of a nonadaptive linear array having the same configuration as the Applebaum type, the output SNR loss is only 6 dB. This technique is based on the assumption that the signal frequency of the desired source is swept across the transmitter bandwidth Δf to generate a two-dimensional voltage vector $V(x, f)$ at the array elements. This signal vector is taken through the different stages of the AFT shown in Fig. 1, to obtain a focused one-dimensional vector $V'(x)$. This signal vector is then fed into the Applebaum array, shown in Fig. 2, where far-field steering is used successfully. The only drawback of the AFT is that it requires a considerable amount of data processing. However, this problem has been eased [8] by the use of a partial convolution in the frequency domain.

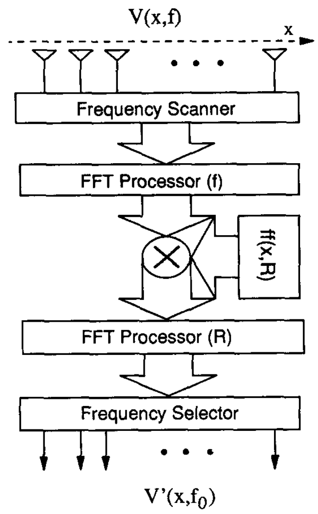

Fig. 1. Direct automatic focusing technique procedure.

II. Problem Formulation

The Applebaum linear array structure [1] considered in this paper is shown in Fig. 2. The N elements are assumed to be isotropic with no mutual coupling. The weights are derived adaptively using *a priori* information [4] in the steering vector to discern the desired signal while suppressing automatically the interference signals. The CW signal is located at (ρ_d, θ_d), where ρ_d and θ_d are the distance and the angle measured from the array center and the broadside direction respectively. In

Manuscript received July 20, 1992; revised December 29, 1992.

A. Yamani is with the King Fahd University of Petroleum and Minerals, Dhahran 31261, Saudi Arabia.

M. Hamiane is with the Faculty of Sciences, Girls Colleges, Dammam, Saudi Arabia.

IEEE Log Number 9211797.

0018-926X/93$03.00

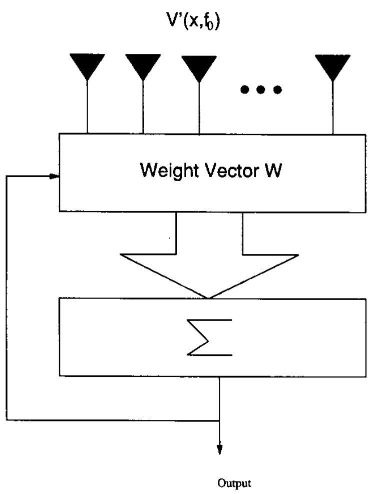

Fig. 2. Applebaum linear array structure.

the steady state, the weight vector $W = (w_1, w_2, \cdots, w_N)^T$ is given by [2]

$$W = M^{-1}S^*, \quad (1)$$

where S^* is the steering vector and the asterisk denotes complex conjugation. M is the covariance matrix, given by

$$M = E\{V^*(t)V^T(t)\}, \quad (2)$$

where $E\{\cdot\}$ denotes the expectation. In (2), $V(t) = (v_1(t), v_2(t), \cdots, v_N(t))^T$ is the input signal vector at the array elements which can be decomposed into

$$V(t) = \alpha(t)S_d + N(t), \quad (3)$$

where $N(t)$ is the noise vector, $\alpha(t)$ is the waveform of the signal, and $S_d = (s_{d_1}, s_{d_2}, \cdots, s_{d_N})^T$ represents the phase components of the signal at the array elements relative to the phase at the origin. The nth element of S_d is given by

$$s_{d_n} = \exp(-jk\rho_n),$$

where $k = 2\pi/\lambda$, $j = \sqrt{-1}$, and ρ_n is the distance from the nth element to the source.

Originally, the AFT was developed for nonadaptive linear arrays where a phase error of $\pi/8$ can be tolerated [5]. Therefore, Fresnel approximation [12] was used successfully for the expression of ρ_n (see Appendix A). To account for the phase sensitivity of the Applebaum array [13], [14], Fresnel approximation is extended to the fourth term of the binomial expansion of ρ_n. It is shown in Appendix A that in the Fresnel region [11] ρ_n can be approximated by

$$\rho_n = \rho_d - x_n \sin\theta_d + \frac{x_n^2 \cos^2\theta_d}{2\rho_d}. \quad (4)$$

Since ρ_d in (4) contributes a constant phase for all array elements, S_d can be written as

$$S_d = \begin{pmatrix} \exp\left[jk\left(x_1 \sin\theta_d - \frac{x_1^2\cos^2\theta_d}{2\rho_d}\right)\right] \\ \exp\left[jk\left(x_2 \sin\theta_d - \frac{x_2^2\cos^2\theta_d}{2\rho_d}\right)\right] \\ \cdots \\ \cdots \\ \exp\left[jk\left(x_N \sin\theta_d - \frac{x_N^2\cos^2\theta_d}{2\rho_d}\right)\right] \end{pmatrix} \quad (5)$$

When the source is in the infinite far field, the quadratic phase term in S_d becomes negligible. The corresponding far-field steering vector $S = (s_1, s_2, s_3, \cdots, s_N)$ where

$$s_n = \exp[jkx_n \sin\theta_d], \quad (6)$$

when used in (1) yields optimal output signal-to-noise ratio. For a value of ρ_d which is less than the far-field range, far-field steering is not applicable [3] and the array needs to be focused at the signal source location (ρ_d, θ_d). For perfect adaptivity, $S = S_d$ and the weight vector given by (1) yields maximum signal-to-noise ratio. In practice, the signal source range information is usually unavailable, and searching for the optimal focusing condition can give rise to an unacceptable degradation in signal-to-noise ratio. Yeh *et al.* [4] derived an approximate expression for the output signal-to-noise ratio (SNR) as a function of the steering distance and the steering angle for an available *a priori* information (ρ, θ) for the signal source location. This is given by

$$\text{SNR} \approx \frac{\gamma_d N}{1 + \gamma_d^2 F(\rho, \theta)}, \quad (7)$$

where $F(\rho, \theta)$ is given in [4]. As a result, a rule of thumb is devised to determine both the steering angle and the steering distance that result in an acceptable SNR loss. It has been shown [4] that these steering parameters must be very close to the exact signal source location, and that the parameters for a conventional beam-forming array cannot be applied directly to the Applebaum array.

III. The Automatic Focusing Technique

The AFT has two versions. The first [7] is based upon a mathematical analysis technique, known as angular spectrum decomposition [9], [10]. It is therefore valid in the very near field, given by [11]

$$\rho \leq \frac{D^2}{2\lambda},$$

where D is the length of the array. The second [6] is based upon the Fresnel formulation of the diffraction field [9]. It is valid in the Fresnel region [11], [12] and extends to the far field. Both versions of the AFT have been validated experimentally in both microwave and ultrasonic regimes [6], [7]. They have produced simultaneous in-focus imagery for point-target reflectors situated at widely different and unknown ranges from the receive aperture plane. In this paper the second version of the AFT is considered. This technique is based on the assumption that the frequency of the signal is swept across the transmitter bandwidth Δf. The received frequency target response for every array element is transformed to the "range" domain through the use of the fast Fourier transform (FFT), where the targets become segregated in the time or "range" domain. A varying Fresnel or focusing factor [8] is used to correct each target at its respective location. The resulting corrected target range response is transformed back to the frequency domain through the use of the inverse fast Fourier transform (IFFT). It has been demonstrated [8] that when the central frequency data are selected, all quadratic defocusing factors due to each target are simultaneously removed. It is demonstrated in this paper that the AFT can focus an Applebaum array whose signal source is located in the Fresnel region at an unknown distance from the center of the array.

IV. Automatic Focusing of Applebaum Array

Focusing an Applebaum array implies the removal of the quadratic phase term

$$\exp\left[-jk\frac{x_i^2\cos^2\theta_d}{2\rho_d}\right], \qquad i \in \text{in } [1,\, N]$$

from (5) and hence from the input signal vector $V(t)$. For simplicity of the analysis, we assume that only the desired signal is present and that the signal amplitude is constant. This approximation is valid since the quadratic phase depends solely on the geometry of the array and the source location $(\rho_d,\, \theta_d)$. Using (3) and (5), the nth array element signal can be written as

$$v_n(t) = v_n = \exp\left[jk\left(x_n\sin\theta_d - \frac{x_n^2\cos^2\theta_d}{2\rho_d}\right)\right]. \quad (8)$$

If the frequency is swept across the transmitter bandwidth, (8) becomes

$$v_n(f) = rect\left(\frac{f-f_0}{\Delta f}\right) \cdot\exp\left[\frac{j2\pi f}{c}\left(x_n\sin\theta_d - \frac{x_n^2\cos^2\theta_d}{2\rho_d}\right)\right], \quad (9)$$

where c is the speed of light. With reference to Fig. 1, the output of the FFT processor $v_n(R)$, where $R = ct$ denotes the range, is corrected by the focusing factor $ff_n(R)$, given by

$$ff_n(R) = \exp\left[jk\frac{x_n^2\cos^2\theta_d}{2R}\right], \quad (10)$$

to yield $v_n'(R)$, the corrected nth array element time or "range" response of the source signal. This signal is taken back to the frequency domain via a second FFT processor to obtain $v_n'(f)$. It is shown in Appendix B that if the center frequency data are selected the quadratic phase term is completely removed and thus

$$v_n'(f_0) = \exp\left[-jk(\rho_d - x_n\sin\theta_d)\right]. \quad (11)$$

In fact, taking the waveform of the signal $\alpha(t)$ and the input noise signal into consideration, the corrected nth array element signal becomes

$$v_n'(t) = \alpha(t)\exp\left[-jk(\rho_d - x_n\sin\theta_d)\right] + n_n(t). \quad (12)$$

Equation (12) is the output of the AFT procedure. It is equivalent to the nth array element voltage due to a source located at an infinite far-field range. Thus, far-field steering can be used in (1) to derive the weight vector that results in the maximum output signal-to-noise ratio, given by

$$\text{SNR}_{\max} = N\gamma_d. \quad (13)$$

However, ρ_d is finite and thus $\delta\rho_n$ given in Appendix A cannot be neglected for any ρ_d in the Fresnel region. The effect of this error on the output SNR is discussed in Section VI.

V. Improvement of the AFT

With reference to the AFT algorithm outlined in Fig. 1, the focused nth array element signal can be written as

$$\begin{aligned} v_n'(f_0) &= F\left[v_n(R)ff_n(R)\right]\big|_{f=f_0} \\ &= v_n(f)\otimes ff_n(f)\big|_{f=f_0}, \end{aligned} \quad (14)$$

where $F[\cdot]$ and $\otimes$ denote the Fourier transformation and the convolution operation respectively. Since the convolution is required only at $f = f_0$, (14) can be further reduced to a simple vector multiplication by putting

$$\underline{v_n}(f) = \begin{pmatrix} v_n(f_1) \\ v_n(f_2) \\ \vdots \\ v_n(f_K) \end{pmatrix}$$

and

$$\underline{ff_n}(f) = \begin{pmatrix} ff_n(f_K) \\ ff_n(f_{K-1}) \\ \vdots \\ ff_n(f_1) \end{pmatrix}$$

where K is the number of frequencies scanned over the bandwidth Δf. Equation (14) becomes

$$v_n'(f_0) = \underline{v_n}(f)^T\underline{ff_n}(f). \quad (15)$$

From (14) and (15), it can be seen that the AFT algorithm has been simplified considerably. The corrected signal is now obtained from the multiplication of the received data as the frequency is scanned and the Fourier transform of $ff(x_n,\, R)$, which can be calculated and stored beforehand. Thus N FFT operations are saved when compared with the direct AFT. This procedure is shown in Fig. 3.

VI. Simulation Results

The AFT has proven its focusing capability experimentally in long-wavelength imaging systems [6] employing nonadaptive linear arrays where a phase error of $\pi/8$ can be tolerated. In this section it is intended to demonstrate its extension to focus adaptive linear arrays such as the Applebaum type. To do this, we assume a 21-element linear array with element spacing equal to $\lambda/2$ ($\lambda = 3$ cm). The signal source is located at $\rho_d = 60\lambda$, which is well within the Fresnel region of a

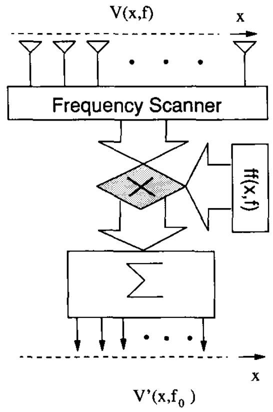

Fig. 3. AFT procedure via the convolution.

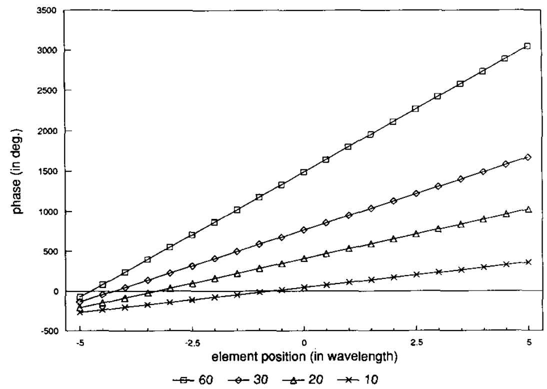

Fig. 5. Phase of $v'(x, f_0)$ versus x for $\rho_d = 60\lambda$, $\theta_d = 10°$, 20°, 30°, and 60°.

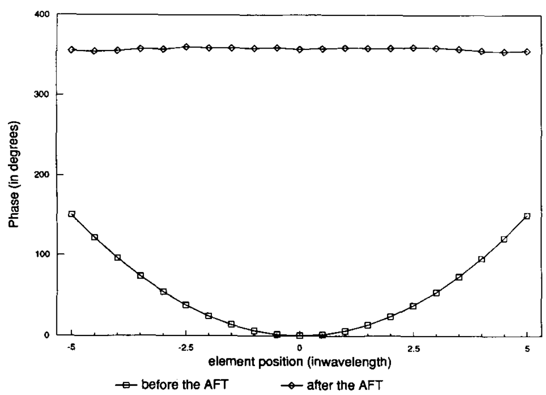

Fig. 4. Phase of $v(x, f_0)$ and $v'(x, f_0)$ for $\rho_d = 60\lambda$, $\theta_d = 0°$.

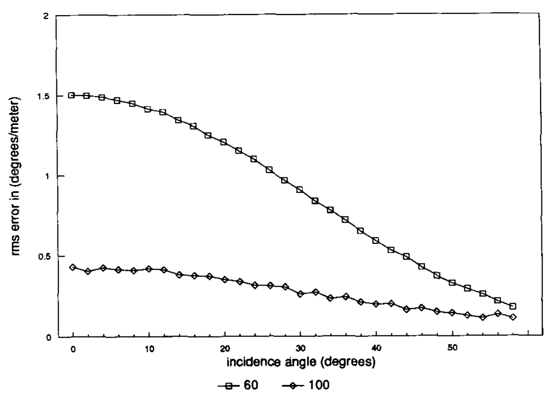

Fig. 6. rms error in the phase slope of $v'(x, f_0)$ versus θ_d for $\rho_d = 60\lambda$ and100λ.

nonadaptive linear array with the same configuration (50λ to 200λ). The AFT assumes a bandwidth $\Delta f = 5\% f_0$ with $K = 21$ frequencies centered at $f_0 = 10$ GHz. The input signal-to-noise ratio per element γ_d is assumed to be 20 dB.

We begin by showing the focusing capability of the AFT. For a source at broadside, Fig. 4 demonstrates clearly that the quadratic phase inherent in the incoming wave is completely removed when the AFT is used.

Next, we show that the focusing capability of the AFT is maintained for any incidence angle, thus confirming the validity of (11). Fig. 5 shows the phase of $v'(x, f_0)$ versus array element position for $\theta_d = 10°$, 20°, 30°, and 60°. It is clear that the phase is linear with element position and that its slope increases with θ_d.

To account for the phase sensitivity of the Applebaum linear array, Fresnel approximation is extended to the fourth terms of the binomial expansion of the expression of ρ_n (see Appendix A). Since the AFT removes solely the quadratic terms in the expression of ρ_n, the phase of $v'(x_n)$ is in fact

$$\phi(x_n) = k(x_n \sin\theta_d + \delta\rho_n),$$

where $\delta\rho_n$ is given by (A3) in Appendix A. For a signal source located at an infinite far field, the slope of $\phi(x)$ is equal to $k \sin\theta_d$. However, when ρ_d is in the Fresnel region, $\delta\rho_n$ cannot be neglected and thus the slope fluctuates around $k \sin\theta_d$. To investigate the importance of these fluctuations, the standard deviation of the phase slope, called here the root mean square (rms) error, is calculated. From (A3) in Appendix A, it can be seen that the rms error in the phase slope is proportional to $\cos^2\theta_d$ and inversely proportional to ρ_d^2. Plots of the rms error in the phase slope versus θ_d and ρ_d are shown in Figs. 6 and 7 respectively. It can be seen from these figures that the rms error decreases rapidly with increasing θ_d and ρ_d and that the maximum rms error is about 1.5° per meter for $\theta_d = 0°$ and $\rho_d = 60\lambda$.

From (10) it can be seen that the focusing factor, $ff(R)$, is independent of ρ_d, this implies that ρ_d generally falls between two successive R samples. Provided that the sampling interval of R is made less than or equal to the smallest range beamwidth, or depth of field, of the Applebaum linear array [4], taken here at $\rho_d = 60\lambda$, the resulting residual quadratic phase error contributes a loss of only 6 dB in the output SNR. As ρ_d is increased, the effect of the residual quadratic phase, although small, on the rms error in the phase slope is visible for large ρ_d. This is shown in Fig. 7. Figs. 8 and 9 show the

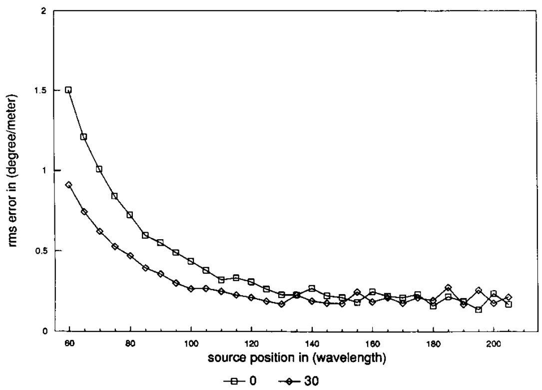

Fig. 7. rms error in the phase slope of $v'(x, f_0)$ versus ρ_d for $\theta_d = 0°$ and 30°.

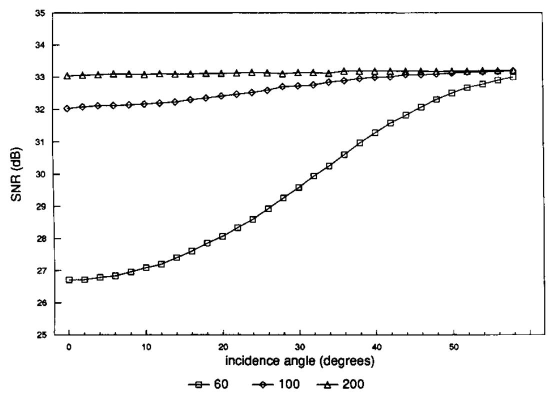

Fig. 8. SNR versus θ_d for $\rho_d = 60\lambda$, 100λ, and 200λ ($N = 21$, $\gamma_d = 20$ dB).

output SNR versus θ_d and ρ_d respectively. As expected, the output SNR is about 6 dB less than $N\gamma_d = 33.22$ dB, for $\rho_d = 60\lambda$ and $\theta_d = 0°$, and increases rapidly with ρ_d and θ_d. For instance, when $\rho_d = 60\lambda$, the output SNR is about 27 dB, whereas when $\rho_d = 100\lambda$ the output SNR is increased to 32 dB.

VII. Conclusion

In this paper we have demonstrated that the AFT can successfully focus an Applebaum linear array whose signal source is located at an unknown distance from the array center. Thereafter, the far-field steering vector can be used successfully.

To account for the phase sensitivity of the Applebaum array, Fresnel approximation is extended so that all quadratic terms in the binomial expansion of the expression of ρ_n are removed by the use of the AFT. The residual phase error due to $\delta\rho_n$ is shown to have little effect on the array output SNR even when the signal source lies at the beginning of the array Fresnel region. Thus, the limitations of the Applebaum linear array when the signal source is not at the far field have been completely removed when the AFT is used. In addition, the exact location of the signal source is not necessary for the AFT to be used provided that the sampling interval of R is made less than or equal to the smallest range beamwidth of the Applebaum linear array.

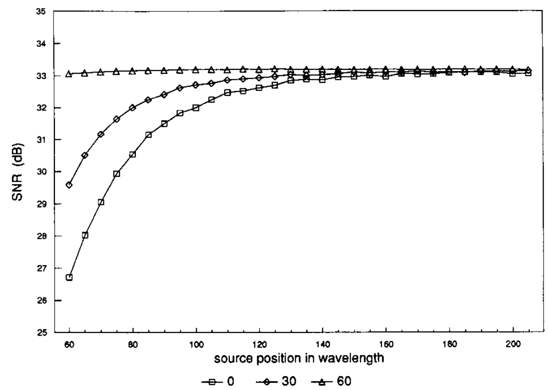

Fig. 9. SNR versus ρ_d for $\theta_d = 0°, 30°$, and $60°$ ($N = 21$, $\gamma_d = 20$ dB).

Finally, the only drawback of the AFT is that it requires a considerable amount of data acquisition and processing. It is possible to improve this technique if the signal source transmits simultaneously all the frequencies instead of scanning them one by one. The received voltage vector $V(x, R)$ can be processed in the same manner as in the original AFT. The "time-domain AFT" performance and implementation will be investigated in the near future.

VIII. Appendix A

In this appendix we derive the expression of the desired signal component at the nth array element. With reference to Fig. 10,

$$\rho_n = \sqrt{(\rho_d - x_n \sin\theta_d)^2 + (x_n \cos\theta_d)^2} = \rho_d\left(1 + \frac{x_n^2 - 2x_n\rho_d \sin\theta_d}{\rho_d^2}\right)^{1/2}. \quad \text{(A1)}$$

In the Fresnel region [11], retaining only the first two terms of the binomial expansion of (A1) for use in the phase component of s_{d_n} is called Fresnel approximation. It is valid [12] for nonadaptive linear arrays. However, Applebaum arrays are very sensitive to phase error and thus Fresnel approximation cannot be used. Retaining the first four terms of the binomial expansion of (A1), it can be shown that

$$\rho_n = \rho_d - x_n \sin\theta_d + \frac{x_n^2 \cos^2\theta_d}{2\rho_d} + \delta\rho_n, \quad \text{(A2)}$$

where

$$\delta\rho_n \approx \frac{\sin\theta_d \cos^2\theta_d}{2\rho_d^2} x_n^3 + \frac{\cos^2\theta_d}{8\rho_d^3}(5\sin^2\theta_d - 1)x_n^4. \quad \text{(A3)}$$

The quantity $\delta\rho_n$ is included to study its effect on the root mean square error in the phase slope of $v'(x)$ covered in Section VI.

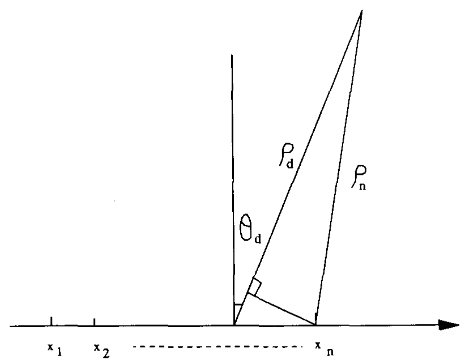

Fig. 10. N-element linear array.

The desired signal component at an arbitrary nth array element is

$$s_{d_n} = \exp - (jk\rho_n) = \exp - \left[jk\left(\rho_d - x_n \sin\theta_d + \frac{x_n^2 \cos^2\theta_d}{2\rho_d}\right)\right]$$

IX. Appendix B
Derivation of Equation (11)

The voltage at the nth array element as the frequency is scanned over Δf is

$$v_n(f) = rect\left(\frac{f - f_0}{\Delta f}\right) \exp - j\left(\frac{2\pi f}{c}\rho_n\right).$$

The inverse Fourier transform of $v_n(f)$ is

$$v_n(R) = \Delta f \exp(jkB(R)) \,\text{sinc}\left[\frac{\Delta f}{c}B(R)\right], \quad \text{(A4)}$$

where

$$B(R) = R - \rho_n \approx R - \rho_d + x_n \sin\theta_d - \frac{x_n^2\cos^2\theta_d}{2\rho_d} \quad \text{(A5)}$$

and

$$\text{sinc}(y) = \sin\frac{(\pi y)}{\pi y}.$$

Upon application of the focusing factor

$$ff_n(R) = \exp\left(j\frac{kx_n^2\cos^2\theta_d}{2R}\right)$$

the corrected nth array element voltage becomes

$$v_n'(R) = \Delta f \exp\left[jk\left(B(R) + \frac{x_n^2\cos^2\theta_d}{2R}\right)\right] \cdot \text{sinc}\left(\frac{\Delta f}{c}B(R)\right). \quad \text{(A6)}$$

It is clear that an exact analytical expression of $v_n'(f)$ cannot be derived due to the $1/R$ term in the phase component of $v_n'(R)$. However, a very close analytical expression can be obtained. Putting

$$l(R) = R - \rho_d + x_n \sin\theta_d \quad \text{(A7a)}$$

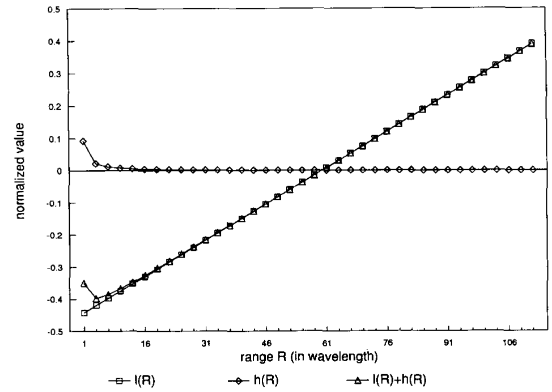

Fig. 11. Variation of $l(R)$, $h(R)$ and $l(R)+h(R)$ versus R for $\rho_d = 60\lambda$, $\theta_d = 0°$.

and

$$h(R) = \left(\frac{1}{R} - \frac{1}{\rho_d}\right)\frac{x_n^2\cos^2\theta_d}{2} \quad \text{(A7b)}$$

such that

$$l(R) + h(R) = B(R) + \frac{x_n^2\cos^2\theta_d}{2R}, \quad \text{(A8)}$$

Fig. 11 shows the variations of $l(R)$, $h(R)$ and $l(R) + h(R)$ in terms of R for $\rho_d = 60\lambda$, $\theta_d = 0°$, and $x = D/2$. It is clear that, from the Fresnel region to the far field, $l(R) \gg h(R)$. Thus $h(R)$ can be neglected in (A8). Using this approximation, the Fourier transform of $v_n'(R)$ becomes

$$v_n'(f) = \frac{\Delta f}{c}\int \exp(jkl(R))\,\text{sinc}\left(\frac{\Delta f}{c}B(R)\right) \cdot \exp - j\left(\frac{2\pi f R}{c}\right) dR. \quad \text{(A9)}$$

Substituting $s = (\Delta f/c)B(R)$ in (A9) yields

$$v_n'(f) = C(x_n, \rho_d, \theta_d) \cdot \int \exp - j\left[\frac{2\pi s}{\Delta f}(f - f_0)\right] \text{sinc}(s)\, ds, \quad \text{(A10)}$$

where

$$C(x_n, \rho_d, \theta_d) = \exp - j\left[\frac{2\pi f}{c}(\rho_d - x_n\sin\theta_d)\right] \cdot \exp - j\left[\frac{\pi x_n^2\cos^2\theta_d}{c\rho_d}(f - f_0)\right] \quad \text{(A11)}$$

and thus

$$v_n'(f_0) = \exp - jk(\rho_d - x_n\sin\theta_d)\int \frac{\sin(\pi s)}{\pi s}\, ds.$$

The value of the integral is a real quantity and thus it does not affect the phase of the signal at the nth array element. For instance, if the integration is taken from ($-\infty$ to $+\infty$)

$$v_n'(f_0) = \exp - jk(\rho_d - x_n\sin\theta_d), \quad \text{(A12)}$$

which is equivalent to the nth array element voltage due to a source located at an infinite far field.

References

[1] S. P. Applebaum, "Adaptive arrays," *IEEE Trans. Antennas Propagat.*, vol. 24, pp. 585–598, Sept. 1976.

[2] S. P. Applebaum and D. J. Chapman, "Adaptive arrays with main beam constraints," *IEEE Trans. Antennas Propagat.*, vol. 24, pp. 650–662, Sept. 1976.

[3] C. C. Yeh, Y. J. Hong, and D. R. Ucci, "The effect of a finite distance source on an Applebaum array," *IEEE Trans. Antennas Propagat.*, vol. 33, pp. 1003–1008, Sept. 1985.

[4] C. C. Yeh, Y. J. Hong, and D. R. Ucci, "The performance of a defocused adaptive array with a finite distance signal source," *IEEE Trans. Antennas Propagat.*, vol. 36, pp. 476–482, Apr. 1988.

[5] B. D. Steinberg, *Principle of Aperture and Array System Design.* New York: Wiley, 1976.

[6] J. C. Bennett and A. Yamani, "Depth of field improvements in long wavelength imaging systems," *Electron. Lett.*, vol. 17, no. 22, pp. 860–862, 1981.

[7] A. Yamani and J. C. Bennett, "Depth of field improvements and removal of distortion in long wavelength imaging systems," *Proc. Inst. Elec. Eng.*, pt. F, vol. 132, no. 3, June 1985.

[8] A. Yamani, "Depth of field improvements and automatic focusing technique in long wavelength imaging systems," PhD. thesis, Sheffield Univ., UK, 1984.

[9] J. W. Goodman, *Introduction to Fourier Optics.* New York: McGraw-Hill, 1963.

[10] E. G. Williams and J. D. Maynard, "Numerical evaluation of the Rayleigh integral for planar radiator using FFT," *J. Acoust. Soc. Amer.*, vol. 72, pp. 2020–2030, 1982.

[11] C. A. Balanis, *Antennas Theory.* New York: Wiley, 1982.

[12] W. H. Southwell, "Validity of the Fresnel approximation in the near field," *J. Opt. Soc. Amer.*, vol. 71, pp. 7–14, 1981.

[13] R. T. Compton, Jr., "Pointing accuracy and dynamic range in a steered beam adaptive array," *IEEE Trans. Aerosp. Elec. Syst.*, vol. 16, pp. 280–287, May 1980.

[14] R. T. Compton, Jr., "The effect of random steering vector errors in the Applebaum adaptive array," *IEEE Trans. Aerosp. Elec. Syst.*, vol. 18, no. 5, pp. 392–400, Sept. 1982.

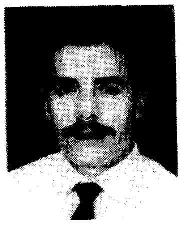

Ahmed Yamani (M'88) was born in El Bayadh, Algeria, on February 15, 1957. He received the B.Eng. degree (first class honors) and a Ph.D. degree, both in electrical engineering, from Sheffield University U.K., in 1981 and 1984 respectively.

From 1984 to 1988 he was a research officer and Head of the Non-Destructive Testing (NDT) Laboratory at the 'Haut Commissariat a la Recherche' (HCR) in Algiers, Algeria. Since 1988 he has been an Assistant Professor at King Fahd University of Petroleum and Minerals, Saudi Arabia. His research interests lie in microwave antennas, long-wavelength imaging systems, signal processing and ultrasound in the field of NDT.

Dr. Yamani is a member of ASNDT.

Madina Hamiane was born in Algiers, Algeria. She received the B.Sc. degree in electronics from the USTHB Algiers in 1979. She then received the M.Sc. degree in cybernetics and a Ph.D. in control engineering from Sheffield University U.K., in 1981 and 1985 respectively.

From 1985 to 1988 she was an Assistant Professor at the USTHB in Algiers. Since 1989 she has been an Assistant Professor at the Girls Colleges, Faculty of Sciences in Dammam, Saudi Arabia. Her research interests encompass multivariables control systems and signal processing.